

Geophysical investigations in the Flumendosa River Delta, Sardinia (Italy) — Seismic reflection imaging

Gian Piero Deidda¹, Gaetano Ranieri¹, Gabriele Uras¹, Pietro Cosentino², and Raffaele Martorana²

ABSTRACT

A geophysical investigation that included seismic-reflection surveying and time-domain electromagnetics (EM) was carried out in the Flumendosa River Delta plain in southeastern Sardinia, Italy. The objective was to improve knowledge of geologic and hydrogeologic controls on a highly productive aquifer hosted in thick Quaternary deposits and known to be affected by an extensive saltwater intrusion. The seismic reflection survey, whose results are reported here, aimed to image the Paleozoic bedrock topography and to obtain detailed structural and stratigraphic information on the sequence of largely fluvial sediments extending from the surface down to bedrock. The survey consisted of two inline profiles, nearly parallel to the coastline and 1 km inland. The sources (0.25 kg of explosives buried at 2 m depth) and receivers (50-Hz vertical geophones) produced a twelvefold data set with common midpoints every 2.5 m. Detailed integrated velocity analysis (constant velocity gathers, constant velocity stacks, and semblance plots) and frequency-wave-number-domain dip moveout (DMO) proved to be the most important processing steps in producing the two stacked sections. Both sections were characterized by distinct seismic units bounded by quasi-continuous reflectors. The lowermost reflection, imaged on section 1 at two-way traveltimes between 310 ms (~300 m) and 580 ms (~530 m) and on section 2 between 200 ms (~190 m) and 65 ms (~52 m), was interpreted to be Paleozoic bedrock. A maximum depth twice as deep as expected was the primary and somewhat surprising result. Imaging of oblique progradational facies — another major finding — proved the existence of undocumented marine Pleistocene sediments that could help in revising the area's geology.

INTRODUCTION

With a rapidly increasing population density, particularly in coastal areas, the quantity and quality of water have become rate-limiting parameters in land management. Proper water-resource management relies on the development of accurate, predictive groundwater-flow models. However, the accuracy of the models is largely dependent upon our ability to determine adequately the geometries of geologic structures and hydrogeologic systems. Groundwater-flow models usually are developed from information obtained by drilling observation wells. However, when geologic settings are complex and/or aquifers are deep, surface geophysical surveys can provide a more economical approach with sufficient detail for modeling.

Among the various geophysical methods, seismic reflection, electric, and EM techniques appear to be the most suitable for this purpose. Seismic reflection profiling potentially can provide an accurate spatial representation of geologic, structural, and stratigraphic boundaries (Birkelo et al., 1987; Jongerius and Helbig, 1988; Geissler, 1989; Miller et al., 1989; Miller and Steeples, 1990; Liberty, 1998; Whiteley et al., 1998). However, electric and EM methods are better suited for identifying hydrogeologic units (Fitterman and Stewart, 1986; Poulsen and Christensen, 1999) and distinguishing between freshwater and saltwater (Mills et al., 1988; Goldman et al., 1991).

Following the general approach reported in Shtivelman and Goldman (2000), a geophysical survey using seismic-reflection and time-domain electromagnetic (TDEM) methods was conducted to study a complex coastal aquifer of vital importance in the southeastern part of Sardinia, Italy. This insufficiently explored study area is the delta plain of the Flumendosa River, which hosts a highly productive aquifer. Unfortunately, the aquifer has been affected by extensive saltwater intrusion caused mainly by uncontrolled overexploitation of groundwater resources for drinking water and irrigation purposes, by fish farming, and by a decrease in natural recharge of coastal aquifers as a result of upstream damming. Detailed knowledge of the ar-

Manuscript received by the Editor February 26, 2005; revised manuscript received June 24, 2005; published online August 7, 2006.

¹University of Cagliari, Dipartimento di Ingegneria del Territorio, Sezione di Geologia Applicata e Geofisica Applicata, Piazza d'Armi, 16, Cagliari 09123, Italy. E-mail: gpdeidda@unica.it; granieri@unica.it; urasg@unica.it.

²University of Palermo, Dipartimento di Chimica e Fisica Della Terra ed Applicazioni Alle Georisorse e ai Rischi Naturali, Via Archirafi 26, Palermo 90123, Italy. E-mail: pietro.cosentino@unipa.it; rafmartorana@libero.it.

© 2006 Society of Exploration Geophysicists. All rights reserved.

ea's geology and hydrogeology is vitally important because prolonged periods of drought have made groundwater the region's predominant (if not sole) water resource.

Generally, quantitative interpretation of subsurface geology requires borehole information. However, because such information is unavailable in the present case, we must rely chiefly on geophysical data for determining the geometry of subsurface structures, with the result that certain aspects remain speculative. Nevertheless, high-quality geophysical imaging can provide detailed, useful subsurface information that cannot be obtained through sparsely spaced drill-holes.

Here, we report the results of a 2D seismic reflection survey designed to image the Paleozoic bedrock topography and to obtain structural and stratigraphic information on the sequence of largely fluvial sediments extending from the surface down to the bedrock boundary. Since we could obtain no certain a priori information about bedrock depth for this location, we assumed a maximum depth of 200–300 m (Di Gregorio, personal communication, 2002), based only on surface geologic and geomorphologic information and bedrock depths from similar areas in Sardinia. The high-quality seismic sections reveal a complex bedrock topography with unexpected maximum depths of about 530 m. The results also show interesting stratigraphic features characteristic of fluvial deltaic environments that could be of great importance for future groundwater exploitation.

SURVEY LOCATION AND GEOLOGIC SETTING

The coastal plain of the Flumendosa River on the southeastern coast of Sardinia (Figure 1) extends from the Tyrrhenian Sea to the village of San Vito (S. Vito), 7 km westward. Prior to this project, little detailed information was available on its geology, despite more than 2000 exploitation wells drilled in the area. In fact, none of these wells, which extend no more than 50 m in depth, sampled the bedrock (Paleozoic) section.

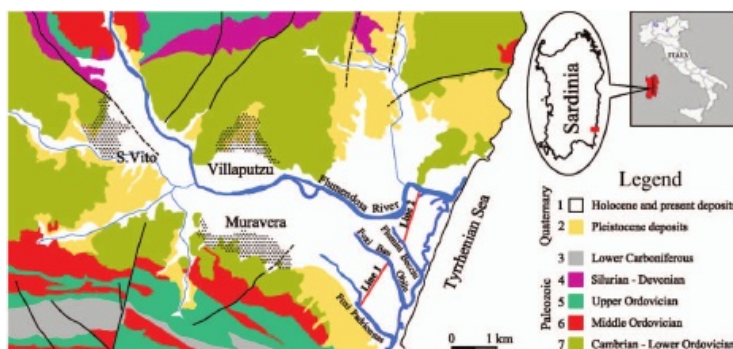


Figure 1. Map showing location of seismic lines and a simplified geology for the Muravera plain survey area. Unit 1: Alluvial (second-order alluvial terraces), colluvial, eolian, and littoral gravels, sand, silt, and clays. Unit 2: Conglomerates and sands forming a system of alluvial terraces (first order) linking up with the Piedmont alluvial fan of detritic material. Units 3–6: Metamorphic rocks (mainly metaconglomerates, metasandstones, metasilstones, metalimestones, and porphyritic metavolcanic rocks) that represent the Paleozoic basement. Unit 7: The Arenarie di S. Vito Formation (irregular sequences of micaceous metasandstones and metaquartzarenites) is the most important outcropping unit bordering the Muravera plain.

The map in Figure 1 is based on surface outcrops of Paleozoic rocks and general geologic features in the area. Schematically, the geology of the area is characterized by a Paleozoic metamorphic basement overlain by a thick Quaternary alluvial blanket. The basement, which outcrops at the edges of the plain, consists of the Paleozoic Arenarie di S. Vito Formation (Cambrian-Ordovician), a thick (>500 m) terrigenous succession of irregular sequences of micaceous metasandstone and metaquartzarenite.

Both Pleistocene and Holocene sediments can be recognized in the Quaternary alluvial deposits. Surface geology and geomorphology, together with bedrock depth information from similar areas, suggest a maximum thickness of 200–300 m for the deposits. Pleistocene sediments are mostly fluvial continental facies, with local marine facies (Tyrrhenian transgression) located slightly south of the area of investigation (Barca et al., 1981). These sediments are comprised of tabular beds of coarse conglomerates with a lean sand-shale matrix that alternates with thin beds of red siltstone. These sediments, which were probably re-incised during the peak of the Würmian marine regression, form a system of alluvial terraces (first order) that outcrop fairly continuously along the banks of the Flumendosa River and its tributaries and link up with Piedmont alluvial fans of detritic material. Holocene alluvial material, largely deposited during the weak Versilian transgression, is comprised of coarse conglomerates with a shaly sand matrix prevailing over pebbles. Afterward, this formation was re-incised, forming a system of second order alluvial terraces that extends throughout much of the plain. A few meters of present alluvial sediments (gravel and sand) complete the Quaternary sequence. Although there are no certain indications of pre-Tyrrhenian marine transgression (Eocene?), the presence of alluvial deposits of that age at the base of the Quaternary sedimentary complex cannot be ruled out (Di Gregorio, personal communication, 2002).

Paleozoic formations in the area are characterized by low-grade metamorphism and two phases of Hercynian tectonics. A system of isoclinal folds with axes striking east-west appears to be related to the first phase, while the folds related to the second phase show axes with a northwest-southeast trend. The main regional fractures (Carmignani et al., 2001) striking east-west and northwest-southeast are normal. Strike-slip faults have resulted in the Cambrian units overlapping the Silurian-Devonian and Carboniferous units (Barca and Maxia, 1982).

A north-south-striking fault system, well known both on dry land and in the continental shelf of southeast Sardinia, is the most important feature of post-Hercynian tectonics. This fault system, associated with Alpine tectonics, has offset the eastern side of the area by about 200–300 m (Calvino, 1961). In particular, these faults, which cut through the Eocene deposits (sandstone and conglomerates) a little farther to the northwest of the surveyed area (Carmignani et al., 2001), could have offset the Eocene deposits themselves in the eastern part, protecting them from complete erosion (Di Gregorio, personal communication, 2002). North-south-striking normal faults, dated to the upper Miocene-Pleistocene, also have been imaged during earlier deep seismic surveys acquired offshore opposite the Muravera plain (Fabretti et al., 1995).

DATA ACQUISITION

The seismic reflection survey includes two P-wave seismic lines, both approximately 1.1 km long (lines 1 and 2 in Figure 1). A few meters above sealevel in the plain, the topography is flat with a maximum elevation variation of only about 0.5 m. Logistical impediments, such as fish farming systems, buildings, and rice fields, prevent the acquisition of a single longline.

For both lines, seismic data were acquired using single 50-Hz geophones attached to a 48-channel seismograph system with 18-bit recording capability. The sample interval was 0.5 ms and the record length 1024 ms (Table 1).

In general, for seismographs that record at 16 bits or more, it is best to record using only a preanalog-to-digital (A/D) antialiasing filter (Steeles et al., 1997). In areas with significant levels of ambient noise or characterized by high-amplitude surface waves, additional low-cut frequency filtering prior to A/D conversion might be advisable. In the present case, a 50-Hz low-cut filter (24-dB/octave roll off) helped to attenuate ground roll better.

Data were recorded using a standard common-midpoint (CMP) roll-along technique in an end-on configuration with 48 active geophones. A 0.25-kg explosive source was buried at approximately 2 m depth (generally below the water table) for each shot position. Geophone spacing of 5 m and source spacing of 10 m provided twelvefold CMP coverage with a CMP spacing of 2.5 m. The maximum source-receiver offset of 245 m was chosen to allow the determination of stacking velocities for reflections from depths of about 200–300 m (e.g., from the expected bedrock surface).

DATA ANALYSIS, PROCESSING, AND RESULTS

The data were generally of high quality, so they required relatively simple processing using commercial software (Table 2). Because noise and signal varied along the lines, shot-record-oriented processing was effective for improving S/N ratio and introduced few computation-related artifacts into the data.

Figure 2 shows shot gathers recorded at three locations along line 1. Reflections are evident above 600 ms. In record 13, the reflection at around 400 ms (event *a*) shows distorted hyperbolic moveout, suggesting a dip-moveout (DMO) effect caused by a downdip reflector. The upper part of record 29 shows clear first breaks followed by reverberating arrivals (event *b*). Finally, record 53 is characterized by low-frequency, high-amplitude ground roll (event *c*). However, note the clear reflection at about 550 ms (event *d*), where reversed moveout suggests an updip reflector at this location.

Figure 3 displays three representative shot gathers recorded along line 2. The S/N ratio for all records along line 2 is less than that for line 1. A

Table 1. Seismic data acquisition equipment and parameters.

Recorder	48-channel Abem Mark 6 seismograph
Energy source	Blasting cap plus 0.25-kg booster
Receivers — single geophones	50 Hz (vertical)
Receivers spacing	5 m
Shot spacing	10 m
Spread geometry	Offend
Minimum offset	10 m
Maximum fold	12
Record length	1024 ms
Time sampling interval	0.5 ms
Analog low-cut filter	50 Hz, 24 dB/octave

Table 2. Seismic data processing sequence.

Data conversion
Geometry
Editing
First-break muting
Spectral analysis and frequency filtering
Predictive deconvolution
Scaling
Velocity analysis
DMO correction
NMO correction
Residual statics
Stack
<i>f-k</i> migration
Time-to-depth conversion

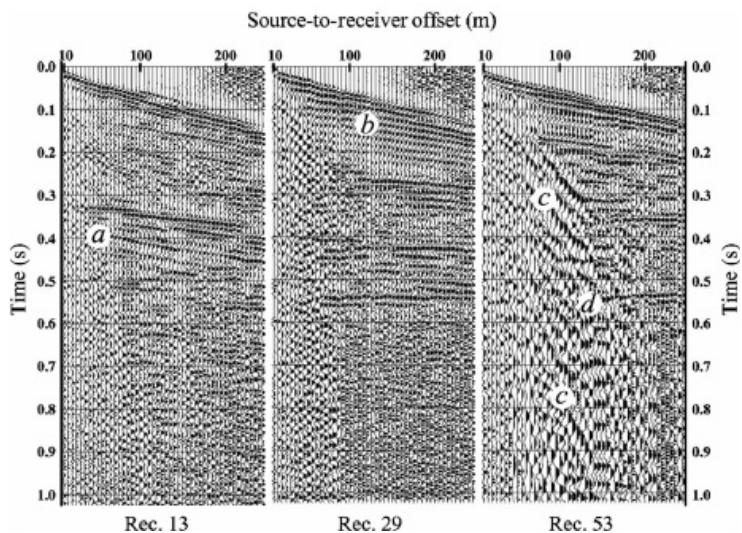


Figure 2. Raw field files from three locations along seismic line 1 (locations indicated by arrows in Figure 5a). For display purposes, automatic gain control (AGC) scaling with a 100-ms window has been applied. Letters *a*, *b*, *c*, and *d* highlight events described in the text.

strong airwave (event *e*) is evident in all records. Event *f*, with clear reversed moveout from record 3 visible up to record 11, suggests the presence of an updip reflector at the beginning of the line, whereas record 72 on the right, representative of records at the end of line 2, shows clearly refracted arrivals *g*, indicating the presence of a reflector at shallower depths.

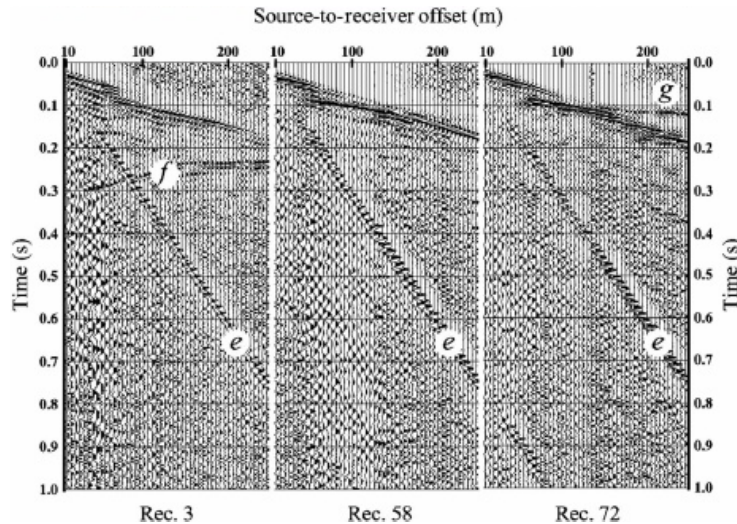


Figure 3. Raw field files from three locations along seismic line 2 (locations indicated by arrows in Figure 6a). For display purposes, an AGC scaling with a 100-ms window has been applied. Letters *e*, *f*, and *g* highlight events described in the text.

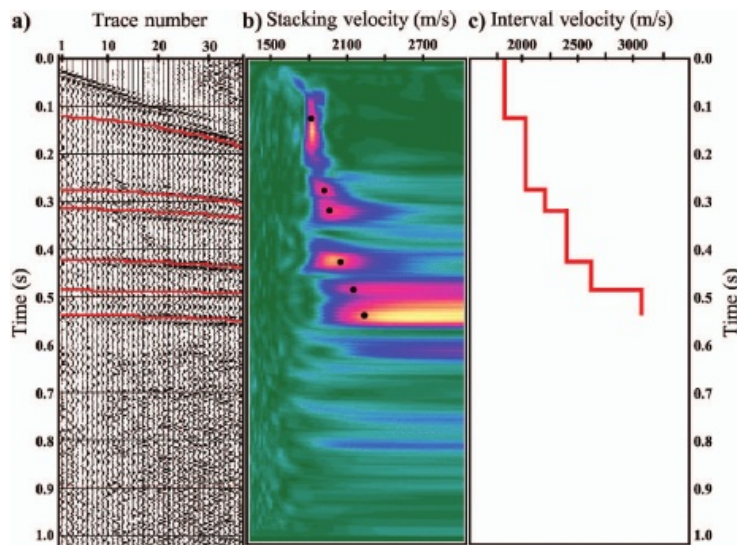


Figure 4. (a) CMP supergather derived from three adjacent CMP gathers along line 1 near the location marked with a black star in Figure 5a. (b) Corresponding semblance analysis showing the estimated velocity function. (c) Interval velocities determined by the Dix equation. Stacking velocities were based on an integrated evaluation of constant velocity gathers, constant velocity stacks, and semblance analysis.

Initial processing steps involved setting up the geometry, followed by routine editing of the entire data set. To avoid misprocessing refractions as reflections, a hand-picked early mute was applied. The reverberations present in some records (such as those observed in record 29 of line 1) were attenuated by predictive-deconvolution filtering. Butterworth filtering (50–180 Hz, 24 dB/octave) helped

attenuate ground roll. Surgical muting was used to remove the airwave from records from line 2.

As is often the case, detailed velocity analysis proved to be the most important and time-consuming processing step. For both lines 1 and 2, the initial velocity models were developed through integrated analysis of constant velocity gathers, constant velocity stacks, and semblance plots. Hand-picked direct arrivals supplied additional information on near-surface velocities. Refracted arrivals, clearly visible in the last records of line 2 (e.g., record 72 on Figure 3), allowed apparent velocity to be measured (4200–7000 m/s) in the upper part of the Paleozoic basement.

As shown by clear reflections in Figure 4a and the relatively sharp peaks in the semblance plot of Figure 4b, resolution of stacking velocities was quite good for events above 500 ms traveltime, while velocity resolution was poor between 500 and 600 ms. Prestack processing was completed with the application of static corrections. Because topography was flat, only residual static corrections were calculated and applied. Five iterations of surface-consistent statics with a maximum allowable shift of ± 5 ms improved the continuity of some events.

To obtain the final stacked-time sections from line 1 (Figure 5a) and line 2 (Figure 6a), further processing was required. Preliminary stacks confirmed the presence of dipping reflectors, as shown in Figure 7 (relative to line 1). To move-out-correct these records properly, dip moveout (DMO) was applied in the f - k domain. Figure 7b shows the improvement from DMO and an improved stacking velocity field. Optimum stacking velocities along lines 1 and 2 are shown in Figures 5b and 6b, respectively.

Finally, applying f - k migration, with input interval velocities obtained by converting stacking velocities in Figures 5b and 6b using Dix equations (Dix, 1955), both DMO-corrected sections were time migrated to obtain the sections in Figures 5c and 6c. Migration was successful where full coverage and detailed velocity models were available. The primary reflecting horizons are clear and can be correlated quite easily with those on the unmigrated time sections.

In general, with a detailed velocity model, migration improves interpretation because the depths of the reflectors can be determined more accurately, scattering is reduced, and dipping reflectors are positioned better. However, the smearing effect of the migration operator could obscure some details and produce artificial align-

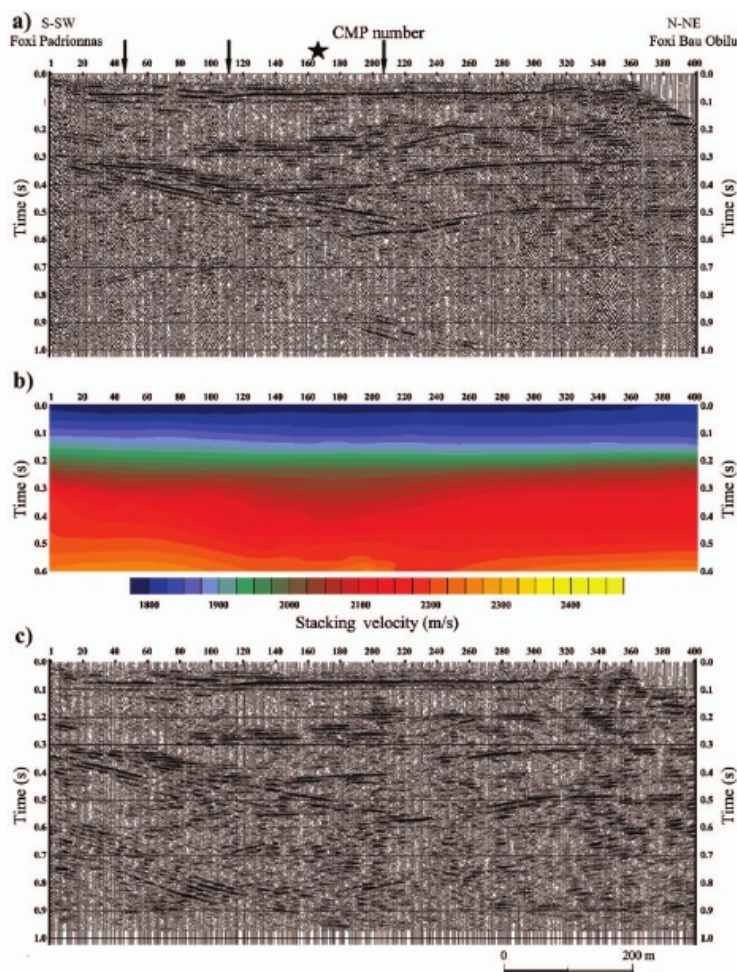


Figure 5. (a) Time section along line 1 (shown in Figure 1). Arrows mark shot positions of raw field files in Figure 2. Black star indicates the position of the CMP supergather in Figure 4. (b) Optimum stacking velocities after dip moveout. (c) An $f-k$ migrated time section obtained from time section in Figure 5a, using an interval velocity field derived from stacking velocities in Figure 5b.

ments. Further problems arise in the present case because the reflectors are too close to the section ends and because, for line 1, the velocities of the deepest reflectors are poorly determined. For these reasons, we based our interpretation on the unmigrated time sections combined with the depth-converted migrated sections.

INTERPRETATION

The preferred interpretations of seismic sections from lines 1 and 2 are displayed in Figures 8 and 9, respectively. For a clearer understanding, the description and interpretation of the sections are discussed separately, because the sections themselves differ substantially. Since no velocity information from boreholes was available in the

investigated area, depth conversion (Figures 8b and 9b) was done based on seismic velocities. Depth sections are relative to sea level, which lies about 2.5 m below the surface.

Reflection line 1

Line 1 begins east of the Paleozoic outcrop at the Foxi Padrionnas bank (Figure 1) and terminates on the right bank of the Foxi Obilu, following a direction parallel to the coastline 1 km inland. The detailed unmigrated seismic section reveals a complex stratigraphic and structural subsurface framework along the survey line (Figure 8). The dominant feature is a reflection visible throughout the entire section, with an apparent dip to the north-northeast, from 310–580 ms two-way traveltime (twtt) between CMP locations 1 and 185 (event α). At CMP locations 133 and 185 (530 and 580 ms twtt, respectively), event α has a bowtie feature (crossing reflections), then dips south-southwest from 580–540 ms twtt with another bowtie feature at CMP location 230. Finally, event α shallows to the end of the line, where it appears nearly horizontal. The bowtie features, together with the general geometry of event α , suggest fault zones may be present around locations 133, 185, and 230. We interpret event α , the deepest coherent reflection, as the top of the Paleozoic basement, whereas the faults marked on the interpreted section might be Hercynian direct faults, striking east-west or northwest-southeast, that fit the regional tectonics and are well documented in the region surrounding the survey area (Carmignani et al., 2001).

Another strong reflection (event β) dominates the right part of the section. It starts from 430 ms twtt, pinches out between locations 125 and 130, and then shallows to 310 ms twtt at the end of the line, similar to event α . The seismic unit C between events α and β is the most difficult to interpret. Because of unit C's great depth (>300

m) and thickness, it is unlikely to be Pleistocene alluvial sediments (in no similar areas of Sardinia have thick units of this type of sediment been documented). Thus, this unit is more likely to be part

of the Eocene deposits cropping out around 10 km northwest of the surveyed area (Carmignani et al., 2001) — deposits lowered eastward by a north-south fault system during the Alpine orogeny. During the Eocene, a vast area in southeast Sardinia, including the surveyed area, was submerged in the sea. Although most of the sediments deposited during this period have been eroded, complete erosion in the study area could have been prevented by Alpine tectonic dislocations (Calvino, 1961). This interpretation suggests that the strong reflection (event β) at the top of unit C might be an erosion surface that formed during the post-Eocene marine regression.

The other well-defined event (event γ) in this section is the shallowest reflection with onset at about 68 ms twtt. Event γ appears as a flat event throughout the entire section, and its position agrees with the boundary between recent (Holocene) and ancient (Pleistocene)

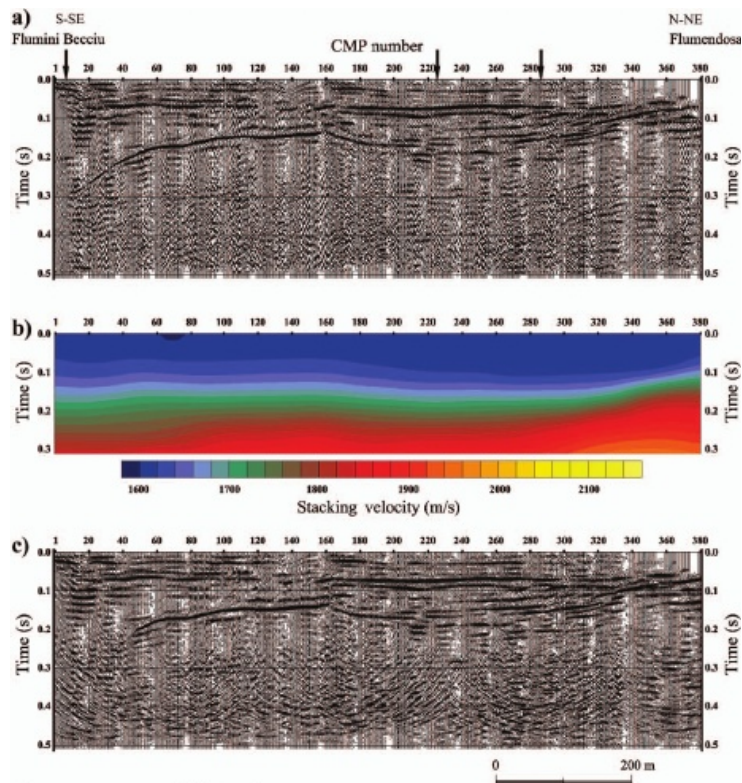


Figure 6. (a) Time section along line 2 (shown in Figure 1). Arrows mark shot positions of raw field files in Figure 3. (b) Optimum stacking velocities after dip moveout. (c) An f - k migrated time section obtained from the time section in Figure 6a using an interval-velocity field derived from stacking velocities in Figure 6b.

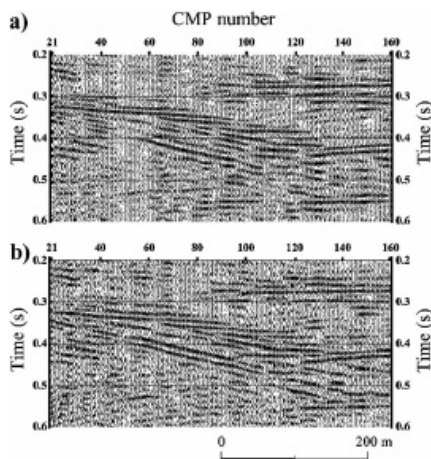


Figure 7. A portion of time section n 1 showing stack improvement (a) before and (b) after DMO processing.

terraced alluvium. Event γ , together with events α in the left portion of the section and β on the right, delimits seismic unit B. Current information suggests this unit is comprised of continental deposits alone, described as ancient (Pleistocene) alluvial deposits.

However, internal reflection patterns (Figure 10) suggest a different interpretation that not only could stimulate geologists to revise the geologic history of the area but also could be useful to better define the groundwater-flow dynamics and to evaluate the quality of groundwater (e.g., brackishwater or saltwater).

Between CDPs 150 and 300, in the time window ranging 200–260 ms twt, oblique progradational facies, characteristic of fluvial deltas and of associated coastal-plain sediments (Sangre and Widmier, 1979), can be observed. These well-mapped, consistent clinoforms probably represent periodic meltins and depositions in a deltaic environment. In other words, during the Pleistocene, a marine sedimentation phase locally replaced the largely continental erosion and deposition processes during an interglacial Riss-Würm transgression (Tyrrhenian II). With interaction of fluvial and marine processes, the Tyrrhenian coastline retreated farther inland for some kilometers, creating a deltaic system in the central part of the plain. The marine conglomerates discovered in the nearby San Priamo plain, 5 km south of the Muravera plain (Barca et al., 1981), testify to a similar situation.

Extending event γ to the surface, seismic unit A is the only unit along the line that was sampled directly by drilling. Unit A consists of Holocene alluvial deposits comprised of conglomerates, sands, and clays. Events appearing in some parts of this section above reflection γ have not been interpreted as genuine reflections. In fact, because the upper 60 ms of the recorded data are generally contaminated by various types of source-generated, high-amplitude noise (direct, refracted, surface waves), it is not always possible to discern reflections and consistently separate coherent noise and signal.

Reflection line 2

Line 2 (see Figure 1) begins on the left bank of the Flumini Becciu channel (500 m from the end of line 1), partially parallels a loop of the Flumendosa River, and terminates on the right bank of the Flumendosa River, 140 m from the Paleozoic outcrop. Two reflections dominate the section in Figure 9. Event α has apparent dip to the north-northeast from about 290–165 ms twt between CMP locations 10 and 60. Then it gently shallows with a dip angle of about 10° , reaching 125 ms twt at CMP 160. In the migrated section the most inclined part of this reflector disappears, suggesting a diffraction (probably a fault) or an artifact of the migration operator caused by low coverage in this part of the section. From CMP 160 to the end of the line, event α is less continuous and has lower amplitudes but

still can be traced across the section. The change in reflection character of event α could be caused by a change in reflectivity of the over-

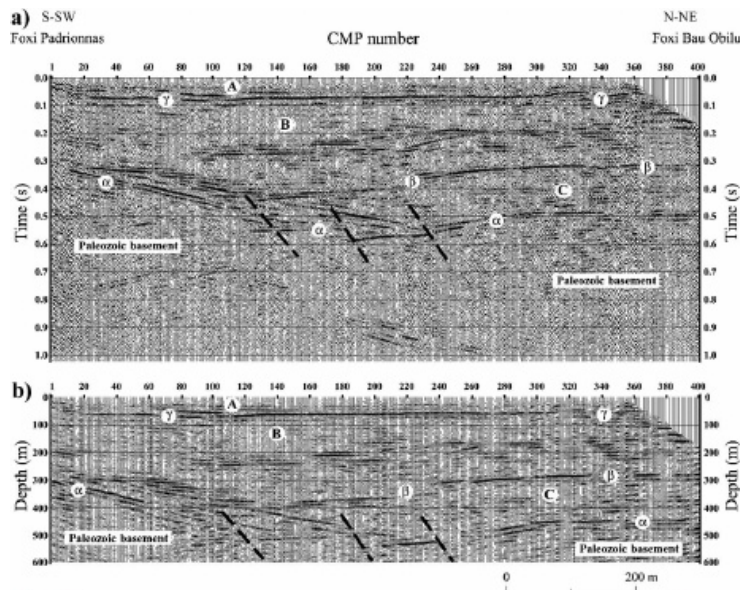


Figure 8. (a) Interpreted time section 1; (b) interpreted depth section 1. Time-to-depth conversion was made using interval velocities obtained using the Dix equation.

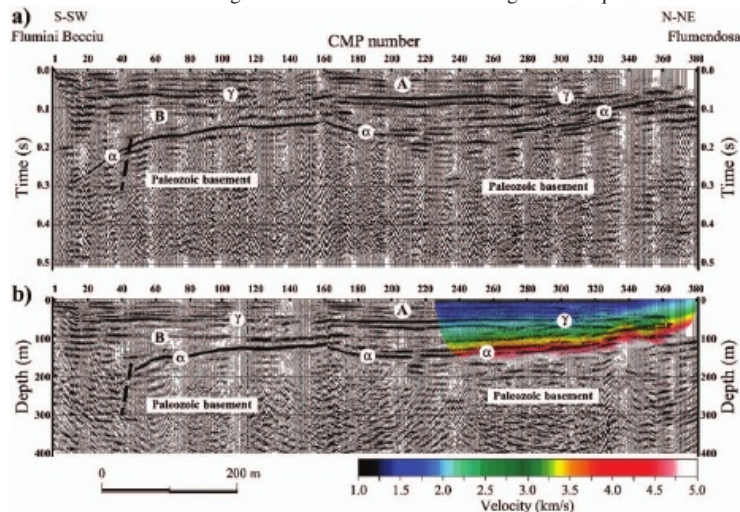


Figure 9. (a) Interpreted time section 2; (b) interpreted depth section 2 with velocity model superimposed. Time-to-depth conversion was made using interval velocities obtained using the Dix equation. The velocity model was obtained by combining reflection-derived interval velocities and tomographic velocities derived from the direct and refracted arrivals. Velocities increase from 1000–3000 m/s in the Quaternary sediments to 3500–4500 m/s in bedrock. Event α is represented by a velocity gradient rather than by a discrete interface in the model because tomography produces smooth models.

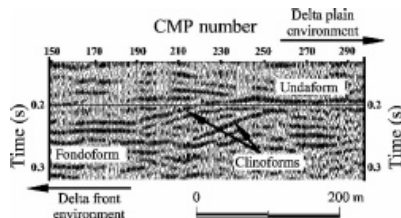


Figure 10. Zoom of time section in Figure 5a showing oblique progradational seismic facies with well-mapped clinoforms characteristic of fluvial delta environments. Undaform zone corresponds to the delta-plain environment. Fondoform zone corresponds to delta-front environment.

lying sedimentary sequence. After an abrupt deepening between CMPs 160 and 200, event α gently updips from 160 ms (~ 135 m) to 130 ms twtt (~ 105 m) at CMP 300. From there, it seems to shallow to the end of the line near the Flumendosa River, reaching 66 ms twtt (~ 52 m).

We interpret event α , which is the deepest coherent reflection in the section, as the top of the Paleozoic bedrock. This interpretation is in good agreement with the outcrop geology and topography. At the end of the section, event α is at a depth of approximately 52 m. By extrapolating it up to the Paleozoic bedrock at the surface, which outcrops 260 m beyond the end of the section, we can tie the subsurface interpretation to the outcrop geology.

The interpretation of event α as the top of the bedrock is also supported by the velocity model obtained by combining reflection-derived interval velocities and those derived from first-arrival information using refraction tomography (Figure 9b). In this velocity model, available only at locations where refracted first breaks are clear, reflector α appears to have velocities from 3500–4500 m/s, which are higher than those obtained from reflections above event α .

Reflection event γ is nearly flat, with onset at 50–70 ms twtt. It extends from the beginning of the line to CMP location 340, where event α pinches out. Event γ probably represents the boundary between Holocene and Pleistocene alluvia. Events above reflection γ were not considered for the same reasons as for line 1.

CONCLUSIONS

The 2D seismic reflection survey carried out in the Muravera plain successfully imaged the subsurface geologic structures of the Flumendosa River Delta. A first-order result of the investigation is the clear image of the Paleozoic basement topography. The > 300 -m maximum depth to the basement beneath profile 1 was somewhat surprising. The deepest part of the basement, at 580 ms twtt (~ 530 m), is nearly twice as deep as expected. Imaging of oblique, progradational seismic facies is another major finding of the investigation. The presence of this seismic pattern, usually characteristic of delta environments, proves that in the Muravera plain, Pleistocene alluvial deposits are partially of marine environment, as are the analogous deposits in the nearby San Priamo plain. This finding is of great importance in better understanding the groundwater-flow dynamics and in guiding other geophysical investigations aimed at improving the knowledge of groundwater quality (saline content) in the area.

Unfortunately, because lithologic controls are

not available, information about the true depth of reflectors and detailed stratigraphic interpretation are unreliable — a problem solvable only through deep-borehole investigations. Despite the inevitable uncertainties on reflector depth and on seismic-unit lithology, the seismic data alone provide a new subsurface model that requires re-interpretation of the geologic history of the area.

The well-defined images we produced prove that the study area is highly conducive to seismic reflection profiling. This will enable more extensive seismic imaging to be conducted throughout the plain, to gather information for constructing a good preliminary subsurface model for other geophysical and hydrogeological investigations. Subsequently, oriented coring will allow us to obtain a detailed geologic interpretation that could be of great help to land and resource managers.

These seismic sections (1) provide conclusive evidence of previously undefined basement topography and (2) image the vertical and lateral extents of the main formations, which could not be obtained through sparsely spaced drillholes. Furthermore, the study demonstrates that the reflection technique can be implemented successfully to provide crucial information for subsurface mapping of structures and stratigraphy in the Muravera plain.

ACKNOWLEDGMENTS

We thank F. Di Gregorio for providing information on the geology of the Muravera plain and M.A. Melis for help in manuscript preparation. We also thank L. Noli, M. Sitzia, M. Serci, A. Lai, and G. Casti for their superlative fieldwork. Timely and helpful reviews by an anonymous associate editor and two anonymous journal reviewers are appreciated. This project (n° 25/98) was partially developed under a grant from the Regione Autonoma della Sardegna (L. R. 9/8/50, n° 43). The support of the University of Cagliari also is acknowledged.

REFERENCES

- Barca, S., F. Di Gregorio, and V. Palmerini, 1981, Linea di costa Pleistocenica nella pianura di S. Priamo (Sarrabus, Sardegna Sud-orientale): *Bollettino della Società Geologica Italiana*, **100**, 71–84.
- Barca, S., and M. Maxia, 1982, Assetto stratigrafico e tettonico del Paleozoico del Sarrabus occidentale, in *Guida alla Geologia del Paleozoico Sardo*: Società Geologica Italiana, 87–93.
- Birkelo, B. A., D. W. Steeples, R. D. Miller, and M. Sophocleous, 1987, Seismic reflection study of a shallow aquifer during a pumping test: *Ground Water*, **25**, 703–709.
- Calvino, F., 1961, Lineamenti strutturali del Sarrabus-Gerrei (Sardegna sud-orientale): *Bollettino del Servizio Geologico d'Italia*, **81**, 489–556.
- Carmignani, L., P. Conti, P. C. Pertusati, S. Barca, N. Cerbai, A. Eltrudis, A. Funedda, G. Oggiano, and E. D. Patta, 2001, Note illustrative della Carta Geologica d'Italia alla scala 1:50000, folio 549 — Muravera: Servizio Geologico d'Italia.
- Dix, C. H., 1955, Seismic velocities from surface measurements: *Geophysics*, **20**, 68–86.
- Fabretti, P., R. Sartori, L. Torelli, N. Zitellini, and G. Brancolini, 1995, La struttura profonda del Margine orientale della Sardegna dall'interpretazione di sismica a riflessione ed a rifrazione: Studi Geologici Camerti, Volume Speciale 1995/2, Convegno Scientifico Nazionale CNR Geodinamica e tettonica attiva del sistema Tirreno-Appennino, 239–246.
- Fitterman, D. V., and M. T. Stewart, 1986, Transient electromagnetic sounding for groundwater: *Geophysics*, **51**, 995–1005.
- Geissler, P. E., 1989, Seismic profiling for groundwater studies in Victoria, Australia: *Geophysics*, **54**, 31–37.
- Goldman, M., D. Gillar, A. Ronel, and A. Melloul, 1991, Mapping of seawater intrusion into the coastal aquifer of Israel by the time domain electromagnetic method: *Geoprospection*, **28**, 152–175.
- Jongier, P., and K. Helbig, 1988, Onshore high-resolution seismic profiling applied to sedimentology: *Geophysics*, **53**, 1276–1283.
- Liberty, L., 1998, Seismic reflection imaging of a geothermal aquifer in an urban setting: *Geophysics*, **63**, 1285–1294.
- Miller, R. D., and D. W. Steeples, 1990, A shallow seismic reflection survey in basalts of the Snake River Plain, Idaho: *Geophysics*, **55**, 761–768.
- Miller, R. D., D. W. Steeples, and M. Brannan, 1989, Mapping a bedrock surface under dry alluvium with shallow seismic reflections: *Geophysics*, **27**, 1528–1534.
- Mills, P., P. H. G. Smith, M. Brown, and L. Evans, 1988, Time domain electromagnetic sounding for mapping sea water intrusion in Monterey County, CA: *Ground Water*, **26**, 771–782.
- Poulsen, L. H., and N. B. Christensen, 1999, Hydrogeophysical mapping with the transient electromagnetic sounding method: *European Journal of Environmental and Engineering Geophysics*, **3**, 201–220.
- Sangree, J. B., and J. M. Widmer, 1979, Interpretation of depositional facies from seismic data: *Geophysics*, **44**, 131–160.
- Shitvelman, V., and M. Goldman, 2000, Integration of shallow reflection seismics and time domain electromagnetics for detailed study of the coastal aquifer in the Nitzanim area of Israel: *Journal of Applied Geophysics*, **44**, 197–215.
- Steeple, D. W., A. G. Green, T. V. McEvilly, R. D. Miller, W. E. Doll, and J. W. Rector, 1997, A workshop examination of shallow seismic reflection surveying: *The Leading Edge*, **16**, 1641–1647.
- Whiteley, R. J., J. A. Hunter, S. E. Pullan, and P. Nutalaya, 1998, "Optimum offset" seismic reflection mapping of shallow aquifers near Bangkok, Thailand: *Geophysics*, **63**, 1385–1394.